A Versatile and Efficient Strategy to Discrete Conjugated Oligomers

Jimmy Lawrence[†‡], Eisuke Goto[†§‡], Jing M. Ren[†], Brenden McDearmon[†], Dong Sub Kim[†], Yuto Ochiai[§], Paul G. Clark[#], David Laitar[#], Tomoya Higashihara[§], and Craig J. Hawker[†*]

[†]Materials Research Laboratory and Departments of Materials, Chemistry and Biochemistry, University of California, Santa Barbara, California, United States. [§]Department of Organic Materials Engineering, Graduate School of Science and Engineering, Yamagata University, 4-3-16, Jonan, Yonezawa 992-8510, Japan. [#]The Dow Chemical Company, Midland, Michigan 48674, United States.

Supporting Information

TABLE OF CONTENTS

Additional Data S2

Figures S2

Experimental Procedures S7

General Information S7

Computational Details S8

Monomer and Oligomer Synthesis S8

Synthesis of 3,4'-dihexyl-2,2'-bithiophene S8

Synthesis of 5'-bromo-3,4'-dihexyl-2,2'-bithiophene S9

Oligomerization of 2-bromo-3-hexyl-5-iodothiophene S10

Oligomerization of 5'-bromo-3,4'-dihexyl-2,2'-bithiophene S10

Oligomerization of 2,7-dibromo-9,9-dioctylfluorene S11

Oligomer separation: parameters for automated gradient chromatography S11

Synthesis of vinyl terminated oligo$(3HT)_6$ S13

Synthesis of D8A S14

Synthesis of D6AD2 ..... S15

Synthesis of D4AD4 ..... S16

Determining the effective conjugation length of oligl(3-hexylthiophene) S17

Time-dependent DFT calculations S18

References S21

Additional Data

Figures

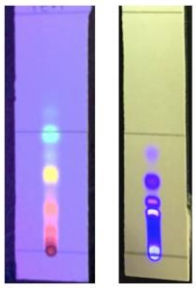

Figure S1. Thin layer chromatography of crude **o3HT$_2$** (left) and oligofluorene samples (right) under UV illumination (eluent: pentane).

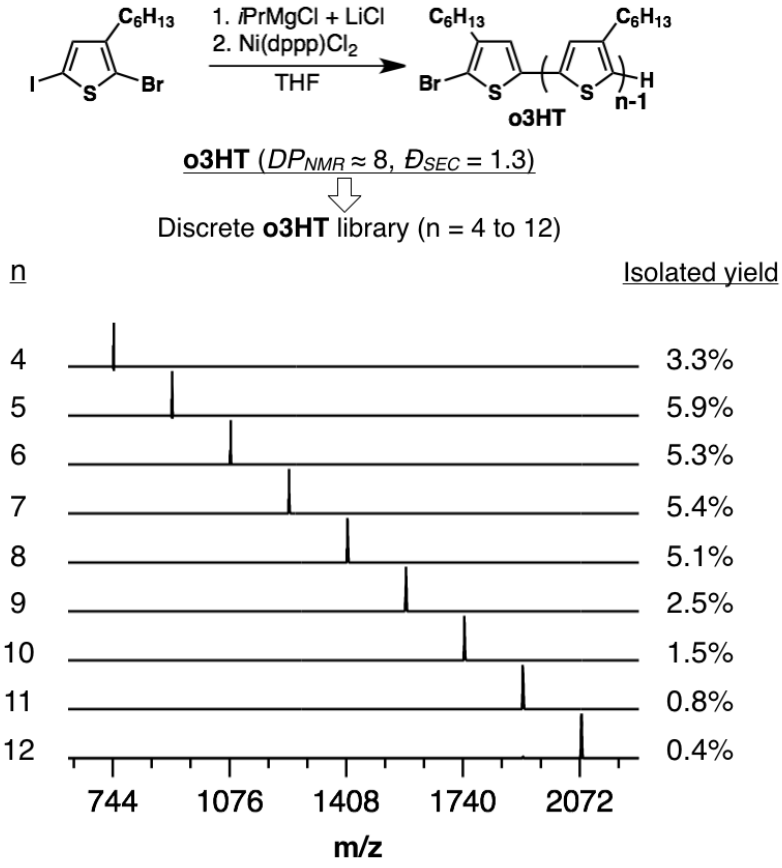

Figure S2. (Top) Synthesis of **o3HT**. (Bottom) MALDI-MS spectra of discrete **o3HT**s (n = 4 to 12) isolated after chromatographic separation and their isolated yields.

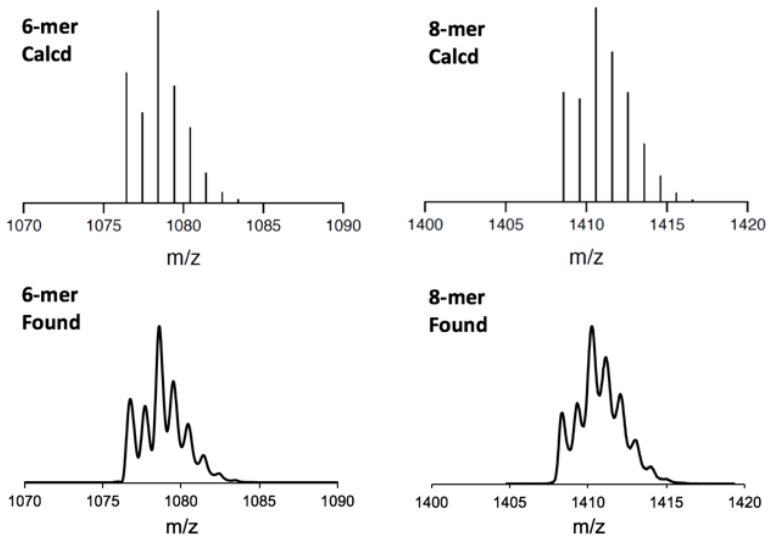

Figure S3. Calculated and observed (MALDI-ToF-MS) isotope patterns of **o3HT** hexamer and octamer.

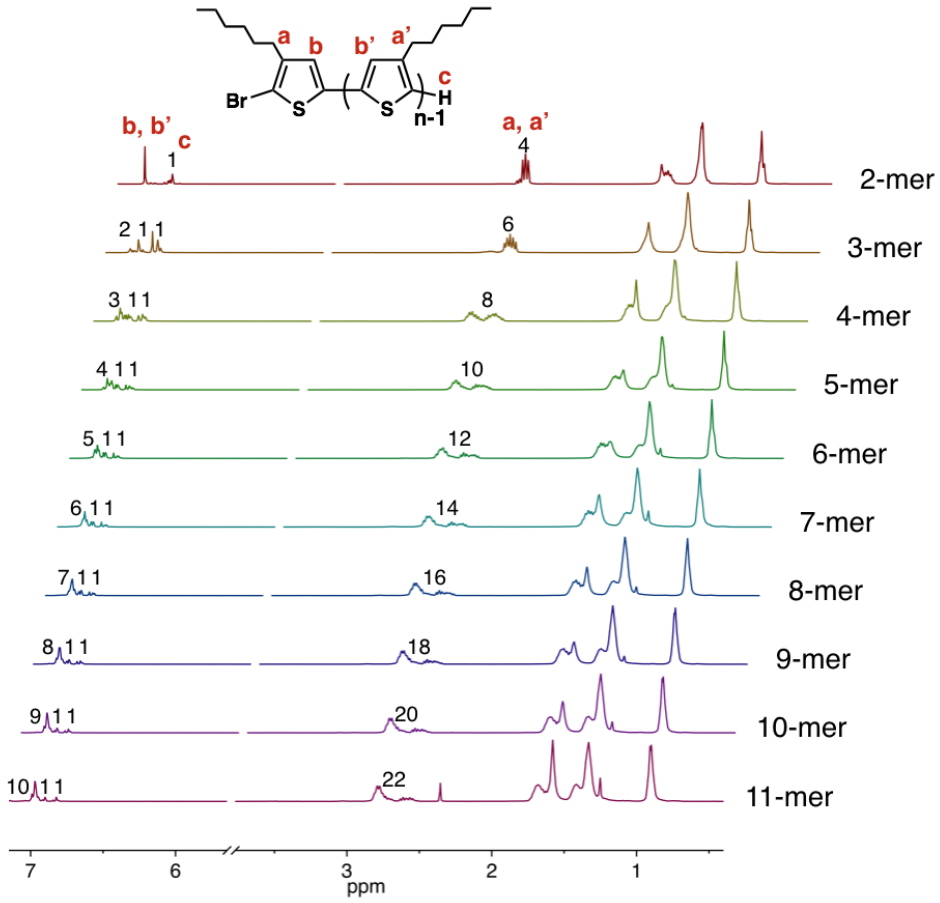

Figure S4. ^{1}H NMR spectra of discrete **o3HT** samples (n = 2 to 11). Integration of the methylene and aromatic protons (*a, a', b,* and *b'*) is normalized to the chain end proton (*c*).

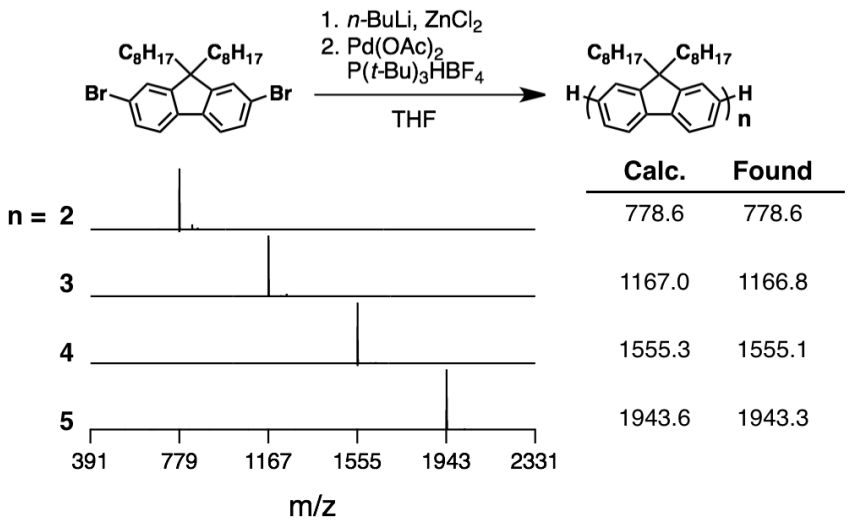

Figure S5. (Top) Synthesis of oligo(9,9-dioctylfluorene) (**oF**). (Bottom) MALDI-MS spectra of discrete **oF**s (n = 2 to 5) isolated after chromatographic separation and their m/z values.

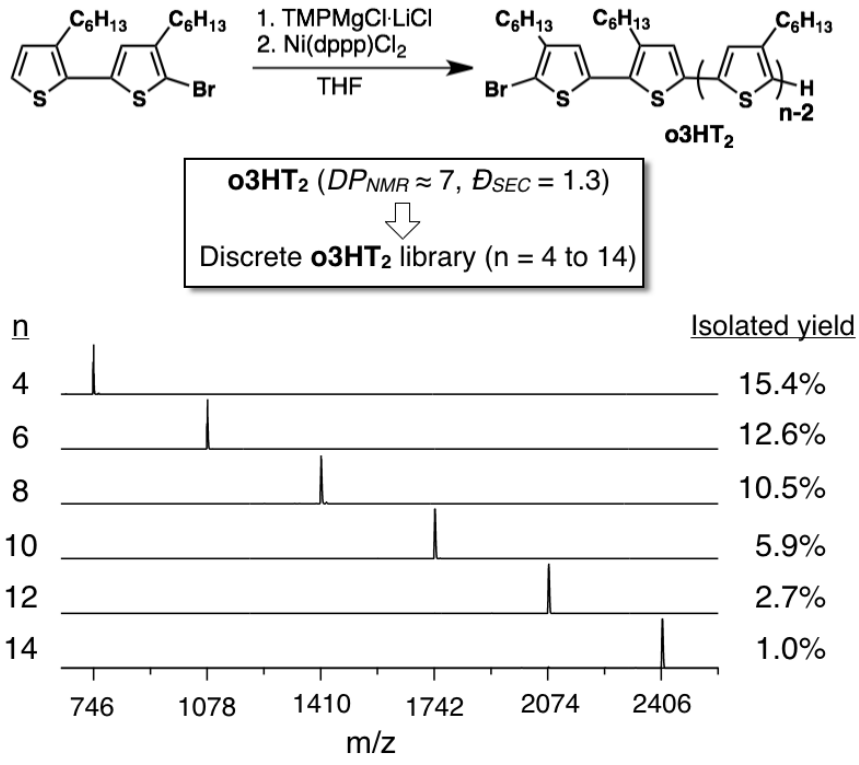

Figure S6. (Top) Synthesis of oligo(3,4'-dihexyl-2,2'-bithiophene) (**o3HT$_2$**). (Bottom) MALDI-MS spectra of discrete **o3HT$_2$** (n = 4 to 14) isolated after chromatographic separation and their isolated yields.

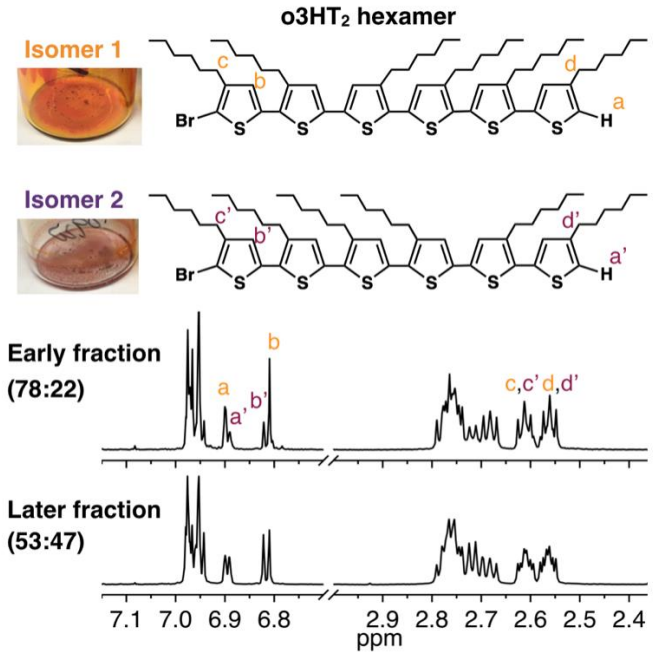

Figure S7. Variation in physical appearance and ^{1}H NMR spectra of **o3HT** hexamer isomers (isomer **1** and **2**). Early fractions of **o3HT** hexamer contains higher content of isomer **1** than the later fractions.

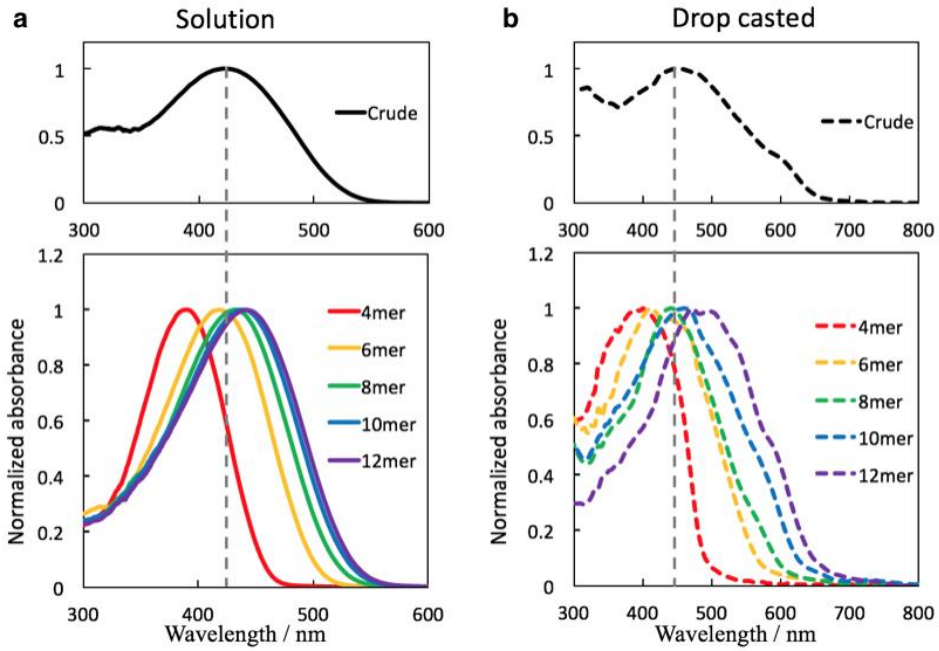

Figure S8. Normalized UV-vis spectra of **o3HT$_2$** samples (a) in chloroform and (b) as drop-casted. Crude disperse samples are shown at the top with discrete samples (4-, 6-, 8-, 10- and 12-mer) shown at the bottom.

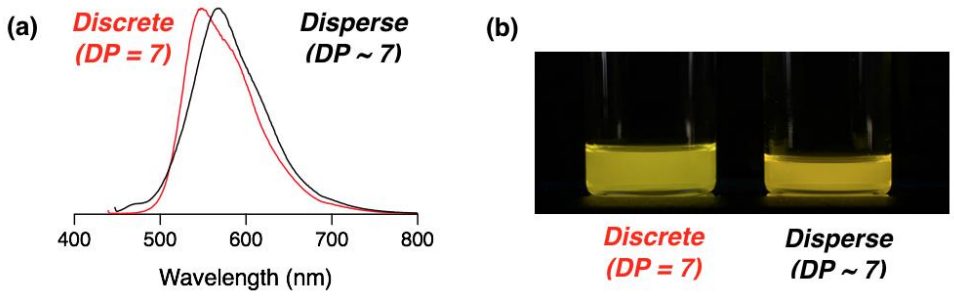

Figure S9. (a) Photoluminescence spectra and (b) fluorescence photographs of discrete ($Đ$ = 1.0) and disperse ($Đ$ = 1.3) **o3HT** heptamer.

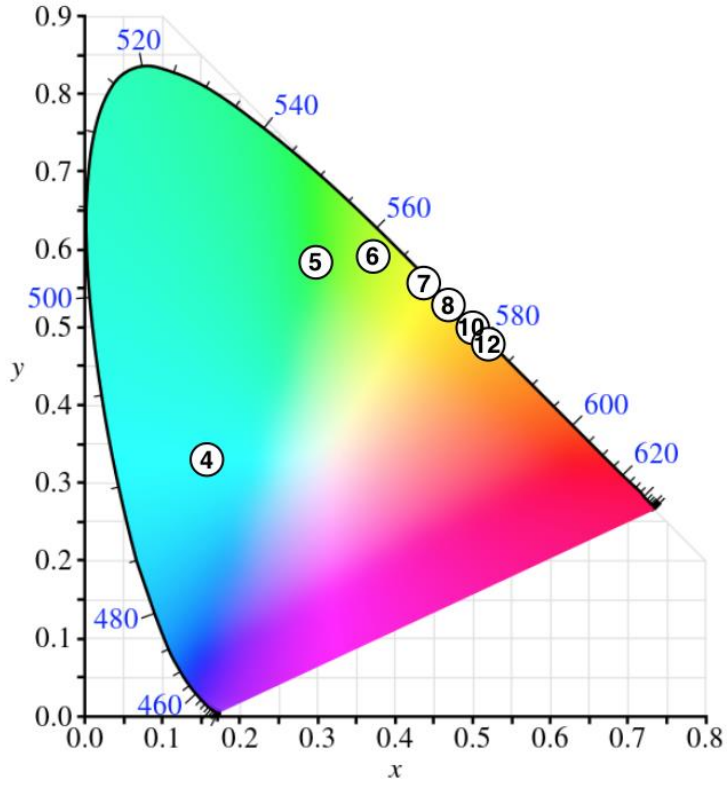

Figure S10. CIE 1931 coordinates of discrete oligothiophenes (n = 4 to 12).

Experimental Procedures

General Information

All reactions were carried out under an inert atmosphere of dry argon in flame-dried glassware, unless the reaction procedure states otherwise. Room temperature reactions were carried out between 21–24 °C. 3-Hexylthiophene, 2-bromo-3-hexylthiophene, 2-bromo-3-hexyl-5-iodothiophene, and 2,7-dibromo-9,9-dioctylfluorene were purchased from Tokyo Chemical Industry and used as received. All other reagents were purchased from Sigma-Aldrich and used without further purification. Anhydrous solvents were taken from a solvent purification system. Automatic flash chromatography of the oligomers was performed on Biotage Isolera unit, using Biotage KP-SIL SNAP/SNAP Ultra cartridge series (25 g/50 g/100 g) eluting with pentane/toluene solvent pairs. Reversed-phase separation was performed using C18-silica gel.

Analytical thin-layer chromatography (TLC) was performed using commercial TLC plates (EMD Millipore) and visualized using combinations of UV, potassium permanganate, ceric ammonium molybdate and iodine staining. ^{1}H and ^{13}C NMR spectra were recorded on a Varian 400, 500, and 600 MHz spectrometer, using the solvent signal for calibration. UV-vis spectra were obtained using Shimadzu UV3600 UV-NIR spectrometer. Photoluminescence spectra were obtained using a Horiba Fluoromax 4 spectrometer. IR spectra were obtained using a Perkins Elmer Spectrum Fourier-Transform Infrared (FTIR) spectrometer. Size exclusion chromatography (SEC) was performed on a Waters 2695 separation module with a Waters 2414 refractive index detector eluting with 0.25 wt% triethylamine/chloroform. Weight average molecular weights (M_w) and number average molecular weights (M_n) were calculated relative to linear polystyrene standards. Reported molecular weights (M_n) were also calculated using ^{1}H NMR by comparing the integration of the protons on the initiating chain end to the polymer pendent groups unless otherwise noted, and by mass spectral analysis. Mass spectral data were obtained at the Mass Spectrometry Facility at the University of California-Santa Barbara, University of California-Irvine and University of California-Los Angeles. MALDI-ToF-MS spectra of oligo(3-hexylthiophene) and oligo(9,9-dioctylfluorene) were taken with and without using dithranol/Na-TFA matrix.

Computational Details

The molecular structures were optimized in vacuum, using the software Avogadro and GaussView 5.0 to enter the starting geometry. Geometry optimizations were carried out using the Gaussian 09 program with the hybrid B3LYP functional and the standard 6-31G(d) basis set. Time-dependent density functional theory (TD-DFT) calculations were performed with the same functional and basis set, and spectroscopic parameters characterizing one-photon excitation spectra and the natural transition orbitals of the compounds were calculated at B3LYP/6-311+G(2d,p) level of theory to obtain simulated UV/vis spectra.

Monomer and Oligomer Synthesis

Synthesis of 3,4'-dihexyl-2,2'-bithiophene[1]

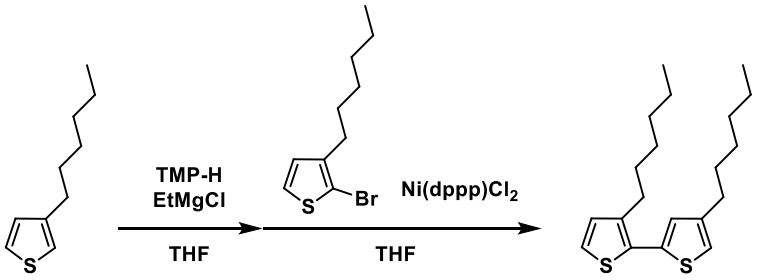

This compound was prepared according to a literature procedure.[1] A 20 mL Schlenk flask was purged with Ar and added with 2.0 M EtMgCl in THF (6.0 mL, 12 mmol) and TMP-H (0.17 mL, 1.0 mmol). 3-hexylthiophene (1.8 mL, 10 mmol) was then slowly added and the reaction mixture refluxed for 24 h. After cooling the reaction mixture to room temperature, anhydrous THF (18 mL), 2-bromo-3-hexylthiophene (2.4 mL, 12 mmol) and Ni(dppp)Cl_2 (110 mg, 0.20 mmol) were added into the flask. The reaction mixture was heated up to 60 ^{o}C and stirred for 21 h, followed by quenching with a saturated NH_4Cl solution (10 mL). The quenched solution was extracted with hexane and washed with DI water. The organic phase was dried over anhydrous magnesium sulfate, rotary evaporated and purified by silica gel chromatography using hexane as eluent to afford the product as a yellow oil (2.7 g, 80%).

^{1}H NMR (600 MHz, $CDCl_3$) δ 7.14 (d, *J* = 5.2 Hz, 1H), 6.95 – 6.90 (m, 2H), 6.88 (m, 1H), 2.74 (t, *J* = 7.8 Hz, 2H), 2.60 (t, *J* = 7.8 Hz, 2H), 1.67 – 1.58 (m, 4H), 1.41 – 1.23 (m, 12H), 0.93 – 0.83 (m, 6H).

^{13}C NMR (100 MHz, $CDCl_3$) δ 143.6, 139.5, 136.0, 131.1, 130.0, 127.4, 123.5, 120, 31.84, 31.80 (2 signals), 30.8, 30.6, 30.5, 29.4, 29.3, 29.2, 22.8, 14.3.

FTIR (ATR, cm^{-1}): 2945, 2915, 2846, 1556, 1525, 1453, 1409, 1373, 1196, 1083, 829, 719.

MS (ESI): $[M+H]^+$ Calcd for $C_{20}H_{30}S_2$: 335.19; Found: 335.03.

Synthesis of 5'-bromo-3,4'-dihexyl-2,2'-bithiophene

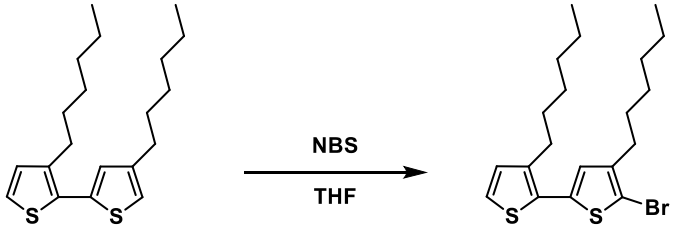

A 20 mL Schlenk flask was added with 3,4'-dihexyl-2,2'-bithiophene (2.91 g, 8.70 mmol) and purged with Ar gas. Anhydrous THF (25 mL) was added and the reaction mixture was cooled down to 0 ^{o}C. Next *N*-bromosuccinimide (1.59 g, 8.90 mmol) was added and the mixture stirred at 0 ^{o}C for 1 h. The reaction mixture was then warmed up to room temperature and stirred for 16 h. The crude mixture was concentrated and dissolved in hexane to remove the residual succinimide by filtration. Removal of the solvent left a crude oil, which was purified by silica gel chromatography using hexane as an eluent to afford the product as a yellow oil (3.5 g, 96%).

^{1}H NMR (600 MHz, $CDCl_3$) δ 7.16 (d, *J* = 5.2 Hz, 1H), 6.91 (d, *J* = 5.2 Hz, 1H), 6.78 (s, 1H), 2.70 (t, *J* = 7.8 Hz, 2H), 2.55 (t, *J* = 7.5 Hz, 2H), 1.66 – 1.56 (m, 4H), 1.41 – 1.21 (m, 12H), 0.94 – 0.82 (m, 6H).

^{13}C NMR (100 MHz, $CDCl_3$) δ 142.5, 140.1, 135.8, 130.1, 130.1, 127.0, 124.1, 108.6, 31.8, 30.9, 29.8, 29.7, 29.3, 29.3, 29.1, 22.8, 14.3.

FTIR (ATR, cm^{-1}): 2945, 2915, 2846, 1556, 1525, 1453, 1406, 1373, 1271, 1256, 1193, 1083, 1004, 829, 762, 748, 721.

MS (ESI) $[M+H]^+$ Calcd for $C_{20}H_{29}BrS_2$: 413.09; Found: 412.94.

Oligomerization of 2-bromo-3-hexyl-5-iodothiophene

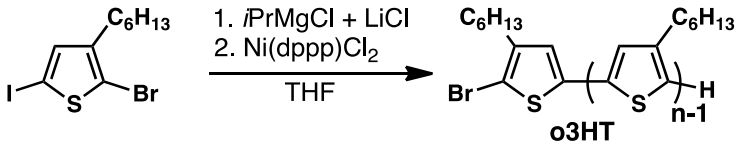

A 200 mL 3-neck flask was added with LiCl (454 mg, 10.7 mmol) and heat gun dried to remove the moisture, then purged with N_2 gas. After 2-bromo-3-hexyl-5-iodothiophene (1.2 mL, 5.4 mmol) and anhydrous THF (120 mL) were added and the mixture cooled down to 0 ^{o}C, *i*PrMgCl (2.0 M in THF, 2.7 mL, 5.4 mmol) was added slowly under stirring at 0 ^{o}C for 20 min. Ni(dppp)Cl_2 (363 mg, 0.670 mmol) was then added at once to start the polymerization. The polymerization was carried out at room temperature for 4 h, followed by quenching using a 5 M HCl solution (10 mL). The quenched solution was poured into a methanol/H_2O solution (750 mL, 2:1 v/v) to precipitate the polymer. After filtration and drying under vacuum, the crude **o3HT** (M_n = 1.7 kDa, $Đ$ = 1.3) was isolated as a sticky, dark purple solid (0.8 g, 87%).

Oligomerization of 5'-bromo-3,4'-dihexyl-2,2'-bithiophene[2]

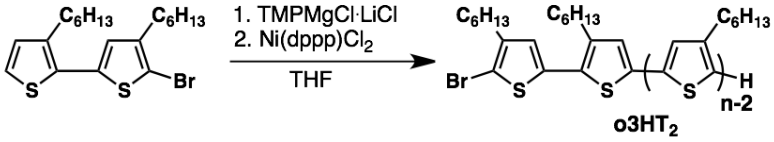

A 250 mL 3-neck flask was added with 1.0 M TMPMgCl·LiCl in THF (6.8 mL, 6.8 mmol) and 5'-bromo-3,4'-dihexyl-2,2'-bithiophene (2.5 mL, 7.0 mmol), purged with a N_2 gas and stirred at room temperature for 3 h. Next anhydrous THF (133 mL) was added and the mixture cooled down to 0 ^{o}C, Ni(dppp)Cl_2 (759 mg, 1.40 mmol) was then added at once to start the polymerization. The polymerization was carried out at room temperature for 4 h, followed by quenching using a 5 M HCl solution (14 mL). The quenched solution was poured into a MeOH/H_2O solution (750 mL, 2:1 v/v) to precipitate the polymer. After filtration and drying under vacuum, the crude **o3HT$_2$** (M_n = 1.7 kDa, $Đ$ = 1.4) was obtained as a sticky, dark purple solid (2.2 g, 95%).

Oligomerization of 2,7-dibromo-9,9-dioctylfluorene[3]

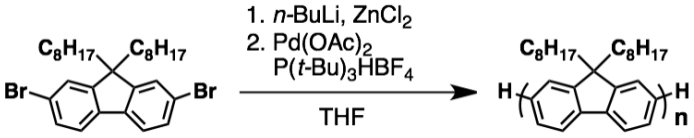

A flame-dried, 200 mL 3-neck flask was added with 2,7-dibromo-9,9-dioctyl-9*H*-fluorene (2.7 g, 5.0 mmol) and transferred into a glovebox. Anhydrous THF (40 mL) was then added and the reaction mixture was cooled to −78 °C. *n*-BuLi (2.6 M solution in hexane, 1.8 mL, 4.8 mmol) was added slowly over 15 min and the mixture was stirred at −78 °C for another 2 h. Next $ZnCl_2$ (0.5 M solution in THF, 10 mL, 5.0 mmol) was added, the mixture warmed up to room temperature over 30 min. A separate oven-dried 20 mL vial was added with $Pd(OAc)_2$ (224 mg, 1.00 mmol) and $P(t\text{Bu})_3HBF_4$ (348 mg, 1.50 mmol), transferred to the glovebox, and added with 10 mL anhydrous THF to dissolve the catalysts. The catalyst solution was then injected swiftly to the flask containing the monomer mixture to initiate the polymerization. The polymerization was carried out at room temperature for 18 h, quenched with 5 M HCl solution (14 mL) and stirred overnight. The quenched solution was poured into a methanol/H_2O solution (750 mL, 2:1 v/v) to precipitate the polymer. After filtration and catalyst removal via Si gel plug and drying, the crude oligofluorene (M_n = 3.6 kDa, $Đ$ = 2.2) was obtained as a sticky, dark green solid (1.6 g, 80%).

Oligomer separation: parameters for automated gradient chromatography

A Biotage Isolera flash purification system was equipped with an appropriate column cartridge (KP SIL or SNAP Ultra, size = 25 g/50 g/100 g).[4] The cartridge (e.g., 100 g) was equilibrated with 3–4 column volumes of the weak solvent. After equilibration is complete, the screw-top cap of the column and the solvent dispersant head insert were detached and set aside. The small volume of remaining solvent was removed, the crude oligomer sample (e.g., 1.5 g) loaded on acid-washed celite was carefully added and packed onto the frit inside the column. Next the screw-top cap was re-attached back and "Gradient" button was pressed to start the elution following a programmed step gradient (Table S1 and S2). The flow rate was set according to the cartridge size, fraction size was set automatically or manually adjusted according to sensor readout.

Table S1. Step gradient profile for oligothiophene separation (normal phase, eluent: pentane/toluene)

%Toluene	Column Volume (CV)
0	8
1	3
2	3
3	3
4	10
5 (purge)	2
5–20 (purge)	1

Table S2. Step gradient profile for oligofluorene separation (normal phase, eluent: pentane/toluene)

%Toluene	Column Volume (CV)
0	4
3	4
6	4
9	4
12	4
15	5
18	5
21	5
21–100 (purge)	1

Representative data for **o3HT** hexamer:

^{1}H NMR (600 MHz, $CDCl_3$) δ 7.03 – 6.88 (m, 6H), 6.86 – 6.79 (m, 1H), 2.88 – 2.48 (m, 12H), 1.74 – 1.56 (m, 12H), 1.47 – 1.26 (m, 36H), 0.96 – 0.84 (m, 18H).

^{13}C NMR (150 MHz, $CDCl_3$) δ 143.8, 143.1, 142.6, 140.0 (3 signals), 139.8, 136.8, 135.6, 134.4, 133.6 (2 signals), 131.2, 130.8, 129.9, 128.8, 128.6, 127.3, 126.8, 126.7, 124.4, 120.2, 107.8, 31.8 (2 signals), 31.8, 30.7 (2 signals), 30.6 (2 signals), 29.9, 29.7, 29.6, 29.4, 29.2, 29.0, 22.8, 14.3.

FTIR (ATR, cm^{-1}): 2953, 2923, 2854, 1520, 1456, 1377, 1198, 1093, 1010, 906, 827, 727.

MS (MALDI-TOF) m/z: $[M]^+$ Calcd for $C_{60}H_{85}BrS_6$ 1076.4; Found 1076.9

Representative data for **o3HT2** hexamer:

^{1}H NMR (400 MHz, $CDCl_3$) δ 6.97 (dd, *J* = 13.0, 5.9 Hz, 5H), 6.90 (d, *J* = 5.7 Hz, 1H), 6.82 (d, *J* = 7.7 Hz, 1H), 2.81 – 2.54 (m, 12H), 1.74 – 1.57 (m, 12H), 1.45 – 1.28 (m, 36H), 0.97 – 0.79 (m, 18H).

^{13}C NMR (150 MHz, $CDCl_3$) δ 143.6, 142.4, 141.7, 140.6, 140.3, 139.7, 139.6, 135.44 and 135.35 (2 signals), 135.0, 134.4, 133.5, 133.4, 131.0, 130.6, 129.8, 129.0, 128.5, 128.4, 128.3, 126.6, 126.3, 125.9, 120.0, 108.6, 31.7, 31.6, 30.5, 30.5, 30.4, 29.7, 29.6, 29.5, 29.4, 29.2, 29.0, 28.9, 22.6, 14.1.

FTIR (ATR, cm^{-1}): 2954, 2924, 2855, 1540, 1521, 1457, 1377, 1200, 1092, 828, 725.

MS (MALDI-TOF) m/z: $[M]^+$ Calcd for $C_{60}H_{85}BrS_6$ 1076.4; Found 1076.5

Representative data for **oF** pentamer:

^{1}H NMR (600 MHz, $CDCl_3$) δ 7.87 – 7.29 (m, 31H), 2.23 – 1.87 (m, 20H), 1.30 – 1.02 (m, 100H), 0.91 – 0.65 (m, 50H).

^{13}C NMR (150 MHz, $CDCl_3$) δ 152.0, 151.2, 140.6, 140.2, 126.9, 126.3, 121.6, 120.1, 55.5, 40.5, 31.9, 30.2, 29.4, 24.1, 22.8, 14.2.

FTIR (ATR, cm^{-1}): 2954, 2925, 2853, 1457, 1404, 1377, 1253, 1000, 906, 885, 813, 738

MS (MALDI-TOF) m/z: $[M]^+$ Calcd for $C_{145}H_{202}$: 1943.6 ; Found 1943.3

Synthesis of vinyl terminated oligo(3HT)$_6$[5]

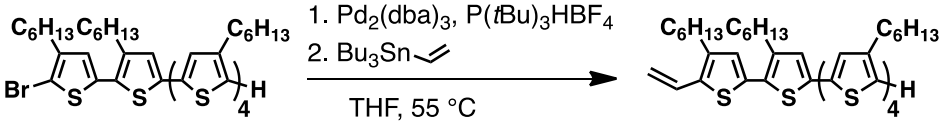

In a glovebox, a 4-mL vial equipped with a stir bar was added with **o3HT$_2$** hexamer (20 mg, 0.018 mmol), dry THF (2 mL) and the mixture stirred for 5 min. The mixture was then added with $Pd_2(dba)_3$ (2.5 mg, 2.8 μmol), P(*t*Bu)$_3$HBF$_4$ (3.2 mg, 0.01 mmol), tributylvinyl tin (50 μL, 0.18 mmol), stirred for 5 min, taken out of glovebox and heated at 55 °C for 12 h. Next the reaction mixture was quenched with aqueous HCl (2 N, 2 mL), extracted with $CHCl_3$, the organic layer washed with water and brine, dried with $MgSO_4$, filtered on celite and concentrated. The dark orange concentrate was precipitated in cold MeOH and centrifuged (5 krpm, 20 min). The precipitate was purified by column chromatography (pentane/DCM) to obtain the target compound as a dark brown solid (11 mg, 60%).

^{1}H NMR (400 MHz, $CDCl_3$) δ 7.17 – 6.64 (m, 7H), 5.51 (dd, *J* = 17.2, 2.2 Hz, 1H), 5.13 (d, *J* = 11.0 Hz, 1H), 2.88 – 2.47 (m, 12H), 1.77 – 1.56 (m, 12H), 1.48 – 1.15 (m, 36H), 0.90 (ddt, *J* = 7.8, 5.3, 2.2 Hz, 18H).

^{13}C NMR (100 MHz, $CDCl_3$) δ 140.5, 140.0, 139.7, 133.8, 131.1, 130.6, 129.0, 128.7, 128.6, 128.1, 127.3, 126.7, 126.0, 120.1, 31.8, 30.7, 29.6, 29.4, 29.2, 22.8, 14.3.

FTIR (ATR, cm^{-1}): 2954, 2924, 2855, 1726, 1455, 1377, 1261, 1215, 1069, 908, 821, 756, 732.

MS (ESI-MS) $[M+H]^+$ Calcd for $C_{62}H_{88}S_6$ 1025.52; Found 1025.98

Synthesis of 4-(octahexyl-octithiophenyl)-benzo[1,2,5]thiadiazole (D8A)

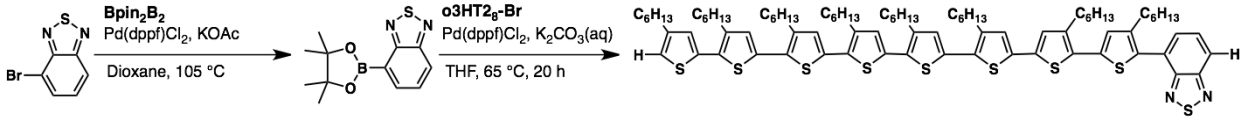

Synthesis of 2,1,3-benzothiadiazole-4-boronic acid pinacol ester (Bpin-BT) The compound was prepared according to literature.[6] A flame-dried, 2-neck Schlenk flask equipped with a stir bar was added with 4-bromo-2,1,3-benzothiadiazole (**4-BT-Br**, 10 mg, 0.047 mmol), bis(pinacolato)diboron (**$Bpin_2B_2$**, 14.2 mg, 0.056 mmol), KOAc (13.3 mg 0.133 mmol), and anhydrous dioxane (1.5 mL). The mixture was purged with Ar for 20 min, and added with $Pd(dppf)Cl_2$ (1.9 mg, 0.0027 mmol) under Ar. The tube was then sealed, stirred at 105 °C and the reaction progress was monitored using TLC. After cooling to r.t., the crude mixture was extracted with diethyl ether (20 mL × 3), washed with saturated sodium bicarbonate, brine, dried over Na_2SO_4 and the solvent evaporated. The product was immediately used in the next step to avoid issues associated with the formation of by-products from protodeboronation.

Suzuki coupling of Bpin-BT and $o3HT2_8$-Br A flame-dried, 2-neck Schlenk flask equipped with a stir bar was added with $o3HT2_8$-Br (40 mg, 0.028 mmol), BPin-BT (12.2 mg, 0.046 mmol), Pd(dppf)Cl2 (3 mg, 0.004 mmol) and subjected to Ar-vacuum cycle three times. Under Ar, the mixture was injected with degassed anhydrous THF (2. 8 mL, purged with Ar for 20 min) followed by degassed $Na_2CO_{3(aq)}$ (1.2 mL, 2 M), sealed and heated at 65 °C under stirring for 20 h. After cooling to r.t., the mixture was extracted with DCM, washed with sodium bicarbonate, brine, dried under Na_2SO4 and the solvent evaporated. The compound was then loaded on acid-washed Celite, and purified by passing through a Si gel column, eluting

with cyclohexane/toluene mixture to remove homocoupled impurities. Further purification to remove polar BT oligomer by-products were achieved by trituration with MeOH or passing the compound through a reversed phase Si plug (MeOH then $CHCl_3$), giving the target product D8A as dark red solid (17% yield after two steps, the purity of fractions to combine was confirmed using MS analysis).

^{1}H NMR (600 MHz, $CDCl_3$) δ 8.02 (d, *J* = 8.6 Hz, 1H), 7.65 (dd, *J* = 18.7, 5.6 Hz, 2H), 7.16 – 6.87 (m, 9H), 2.89 – 2.55 (m, 16H), 1.76 – 1.60 (m, 16H), 1.49 – 1.16 (m, 48H), 0.97 – 0.81 (m, 24H).

^{13}C NMR (151 MHz, $CDCl_3$) δ 155.3, 154.1, 143.8, 142.2, 140.5, 140.5, 140.0, 139.9, 139.8, 136.4, 136.3, 135.6, 134.9, 134.8, 133.9, 130.7, 130.0, 129.5, 128.7, 128.0, 127.3, 126.7, 121.0, 120.2, 31.8, 31.7, 30.7, 29.6, 29.4, 22.8, 22.7, 14.3, 14.2.

FTIR (ATR, cm^{-1}): 2953, 2922, 2853, 1636, 1521, 1486, 1456, 1377, 1260, 1201, 1158, 1091, 852, 825, 807, 753, 725.

MS (MALDI-TOF) m/z: $[M]^+$ Calcd for $C_{86}H_{116}N_2S_9$ 1464.7; Found 1464.6

Synthesis of 4-(dihexyl-bithiophenyl)-7-(hexahexyl-sexithiophenyl)-benzo[1,2,5] thiadiazole (D6AD2)[4]

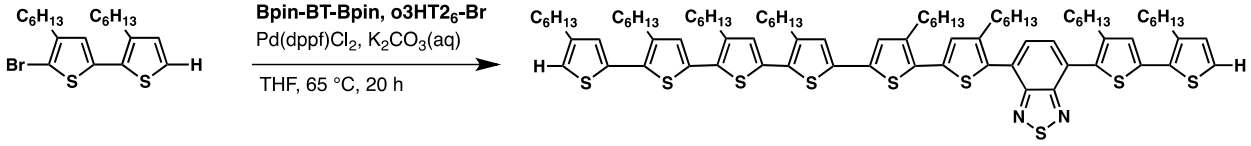

A flame-dried, 2-neck Schlenk flask equipped with a stir bar was added with 03HT2_6-Br (40 mg, 0.037 mmol), 03HT2_2-Br (17 mg, 0.037 mmol), BPin-BT-BPin (14 mg, 0.036 mmol), Pd(dppf)Cl2 (3 mg, 0.004 mmol) and subjected to Ar-vacuum cycle three times. Under Ar, the mixture was injected with degassed anhydrous THF (2. 8 mL, purged with Ar for 20 min) followed by degassed $Na_2CO_{3(aq)}$ (1.2 mL, 2 M), sealed and heated at 65 °C under stirring for 20 h. After cooling to r.t., the mixture was extracted with DCM, washed with sodium bicarbonate, brine, dried under Na_2SO_4 and the solvent evaporated. The compound was then loaded on acid-washed Celite, and purified by passing through a Si gel column, eluting with cyclohexane/toluene mixture to remove homocoupling impurities (D6AD6). Further purification to remove polar BT oligomer and coupling by-products (D2AD2) were achieved by passing the compound through a

reversed phase Si plug (MeOH then $CHCl_3$), to isolate the target product D2AD6 as dark red solid (10% yield, the purity of fractions to combine was confirmed using MS analysis).

^{1}H NMR (600 MHz, $CDCl_3$) δ 7.72 (d, *J* = 25.3 Hz, 2H), 7.25 – 6.74 (m, 7H, overlapped signals), 2.86 – 2.56 (m, 16H), 1.75 – 1.60 (m, 16H), 1.47 – 1.15 (m, 48H), 0.97 – 0.81 (m, 24H).

^{13}C NMR (201 MHz, $CDCl_3$) δ 154.2, 153.9, 143.2, 142.3, 141.0, 139.9, 139.7, 136.9, 130.7, 130.2, 130.0, 129.9, 128.1, 127.3, 126.8, 124.9, 123.9, 31.8, 30.8, 29.9, 29.4, 22.79 and 22.75 (2 signals), 14.3, 14.2.

FTIR (ATR, cm^{-1}): 2955, 2922, 2852, 2359, 1727, 1642, 1530, 1461, 1377, 1260, 1159, 1092, 1022, 907, 875, 802, 731.

MS (MALDI-TOF) m/z: $[M]^+$ Calcd for $C_{86}H_{116}N_2S_9$ 1464.7; Found 1464.9

Synthesis of 4,7-bis(tetrahexyl-quarterthiophenyl)-benzo[1,2,5]thiadiazole (D4AD4)[4]

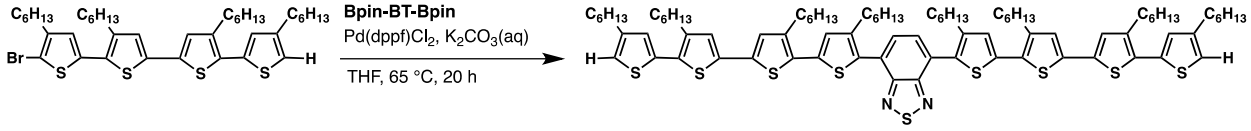

A flame-dried, 2-neck Schlenk flask equipped with a stir bar was added with 03HT2$_4$-Br (40 mg, 0.054 mmol), BPin-BT-BPin (14 mg, 0.036 mmol), Pd(dppf)Cl_2 (3 mg, 0.004 mmol) and subjected to Ar-vacuum cycle three times. Under Ar, the mixture was injected with degassed anhydrous THF (2. 8 mL, purged with Ar for 20 min) followed by degassed $Na_2CO_{3(aq)}$ (1.2 mL, 2 M), sealed and heated at 65 °C under stirring for 20 h. After cooling to r.t., the mixture was extracted with DCM, washed with sodium bicarbonate, brine, dried under Na_2SO4 and the solvent evaporated. The compound was then loaded on acid-washed Celite, and purified by passing through a Si gel column, eluting with cyclohexane/toluene mixture to remove homocoupled and byproduct impurities. Further purification to remove polar BT oligomer and traces of impurities were achieved by passing the compound through a reversed phase Si plug (MeOH then $CHCl_3$), to isolate the target product D4AD4 as dark red solid (26% yield, the purity of fractions to combine was confirmed using MS analysis).

^{1}H NMR (600 MHz, $CDCl_3$) δ 7.70 (s, 2H), 7.20 – 6.79 (m, 9H), 2.89 – 2.50 (m, 16H), 1.77 – 1.60 (m, 16H), 1.47 – 1.11 (m, 48H), 0.98 – 0.81 (m, 24H).

^{13}C NMR (151 MHz, $CDCl_3$) δ 154.2, 143.8, 142.3, 140.5, 140.2, 136.7, 135.7, 135.1, 134.7, 132.2, 130.3, 130.2, 129.8, 129.7, 128.0, 127.3, 126.6, 120.1, 31.8, 30.7, 29.8, 29.4, 28.2, 22.8, 22.7, 14.3, 14.2.

FTIR (ATR, cm^{-1}): 2953, 2923, 2854, 1637, 1534, 1457, 1377, 1189, 1094, 874, 832, 725.

MS (MALDI-TOF) m/z: $[M]^+$ Calcd for $C_{86}H_{116}N_2S_9$ 1464.7; Found 1464.9

Determining the effective conjugation length of oligo(3-hexylthiophene)

Following the analysis described by Briseno and co-workers,[7] the effective conjugation length (n_{ecl}) of **o3HT** was found to be 14-mer. n_{ecl} was calculated from fitting the wavelength of absorbance maximum ($\lambda_{max}(n)$) with the repeating units (n) to the equation below (n_{ecl} = 14.2, λ_∞ = 442.4 nm λ_1 = 271.0 nm, b = 0.390, R^2 = 0.998).

$$\lambda_{max}(n) = \lambda_\infty - (\lambda_\infty - \lambda_1)e^{-b(n-1)}$$

$$n_{ecl} = \frac{\ln(\lambda_\infty - \lambda_1)}{b} + 1$$

Similar result for n_{ecl} with near-ideal correlation (R^2 ~ 1) was obtained when emission maxima was used, presumably due to the well-defined emission spectra of the discrete samples.

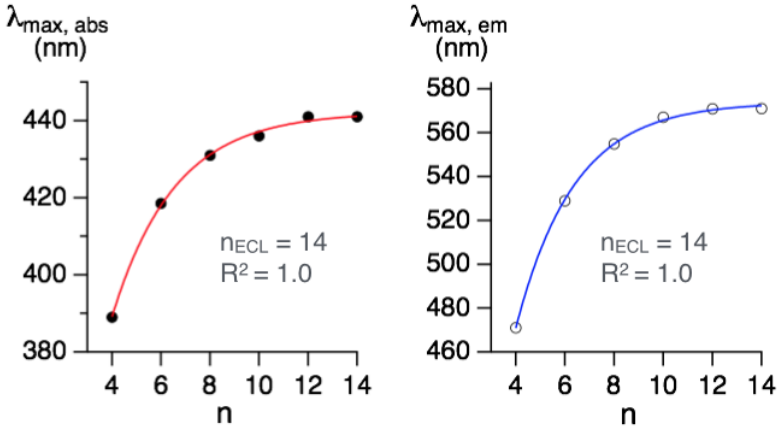

Figure S11. Left: Correlation between the wavelength of maximum absorbance ($\lambda_{max, abs}$) of **o3HT** samples and their degree of polymerization (n). Right: Correlation between the wavelength of maximum emission

($\lambda_{max, em}$) of **o3HT** samples and their degree of polymerization (n). Note: identical n_{ECL} and R^2 values were obtained when n= 2 to 12 were used in the fitting.

Time-dependent DFT (TD-DFT) calculations

Theoretical calculations were performed on the simplified forms of the compounds (methyl instead of hexyl side chains, D8A*, D6AD2* and D4AD4*). Following their geometry optimization (B3LYP/6-31G(d)), TD-DFT calculations were performed to calculate the first 10 singlet excited state transitions at the same level of theory. The simulated UV/vis spectra were calculated from these first 10 excitations, where the splitting of absorbance was observed as the BT unit shifts from the chain end toward the center of backbone (Figure S12). All transitions with oscillator strength greater than 0.4 were further analyzed by calculating their corresponding natural transition orbitals (NTO, B3LYP/6-311+G(2d,p)). In Figure S13–S15, NTO analysis showing the donor-to-acceptor transition were labelled with "A", and the transition to quinoid-like state and other mixed states were labelled with "B" and "C", respectively. In the case of D6AD2, two donor-to-acceptor transitions were observed and labelled as "A1" and "A2".

Interestingly, the calculation of these symmetric and asymmetric materials clearly showed the impact of acceptor placement on their optoelectronic properties. As observed experimentally, the calculated UV/vis spectra of D8A is unimodal, and the spectra profile of D6AD2 is slightly bimodal, where the λ_{max} for D6AD2 blue-shifted relative to that of D8A, but the λ_{onset} of D6AD2 is red-shifted relative to that of D8A (Figure S12). The calculated UV/vis spectra for the symmetric D4AD4 is bimodal with the lower energy donor-to-acceptor transition ("A") having lower oscillator strength than the higher energy aromatic-to-quinoidal-type transition ("B"). The natural transition orbital analysis for these structures showed that in comparison to the major transitions of the symmetric D4AD4, the major transitions in D8A and D6AD2 are split and mixed types due to their structural asymmetry.

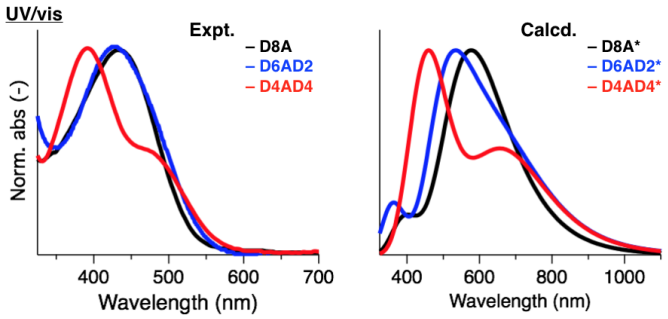

Figure S12. Comparison between UV/vis spectra measured for D8A, D6AD2 and D4AD4 and their simulated UV/vis spectra (B3LYP/6-31G(d)//B3LYP/6-311+G(2d,p))

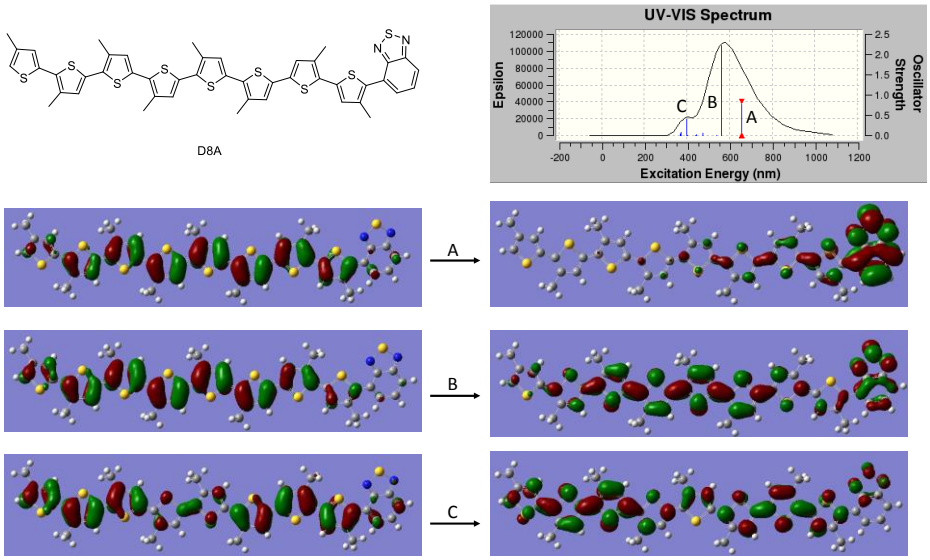

Figure S13. The simulated UV/vis spectra and Natural Transition Orbital analysis of D8A*. The lowest energy transition (A) is a donor-to-acceptor charge transfer transition. The second transition (B) is a mixture of donor-to-acceptor charge transfer transition and aromatic-to-quinoidal type transition. The third transition (C) is an aromatic-to-quinoidal type transition localized primarily on the donor.

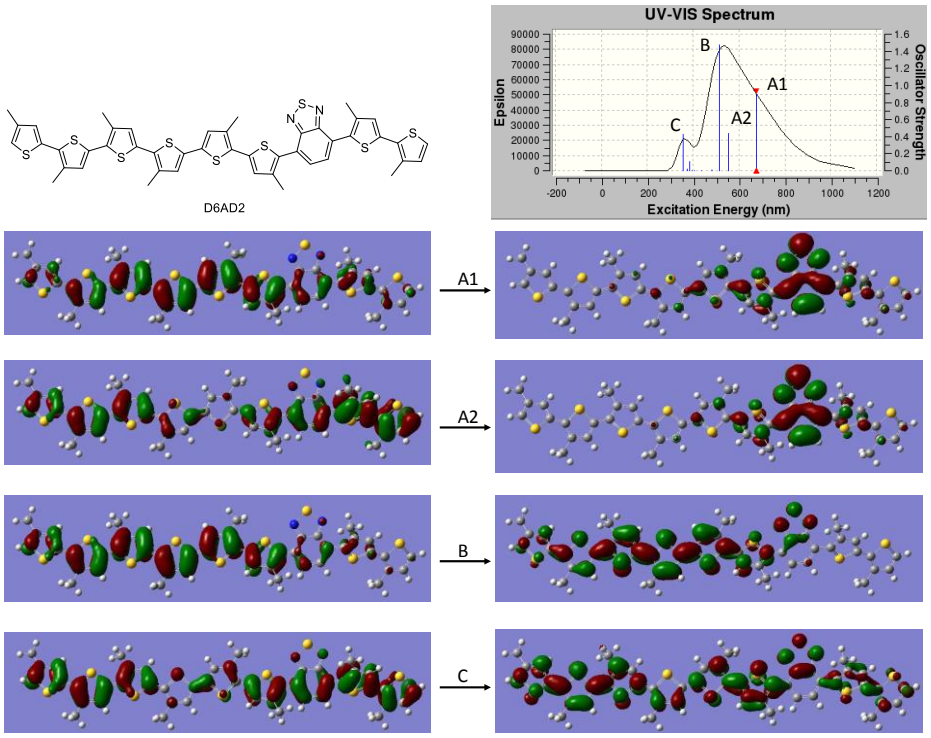

Figure S14. The simulated UV/vis spectra and Natural Transition Orbital analysis of D6AD2*. The first transition (A1) is a donor-to-acceptor charge transfer transition (D6 to A). The second transition (A2) is also a donor-to-acceptor charge transfer transition with more contribution from the dimer donor. The third (B) and fourth transition (C) are predominantly aromatic-to-quinoidal type transitions, with the dimer contribution being more significant in transition C than in transition B.

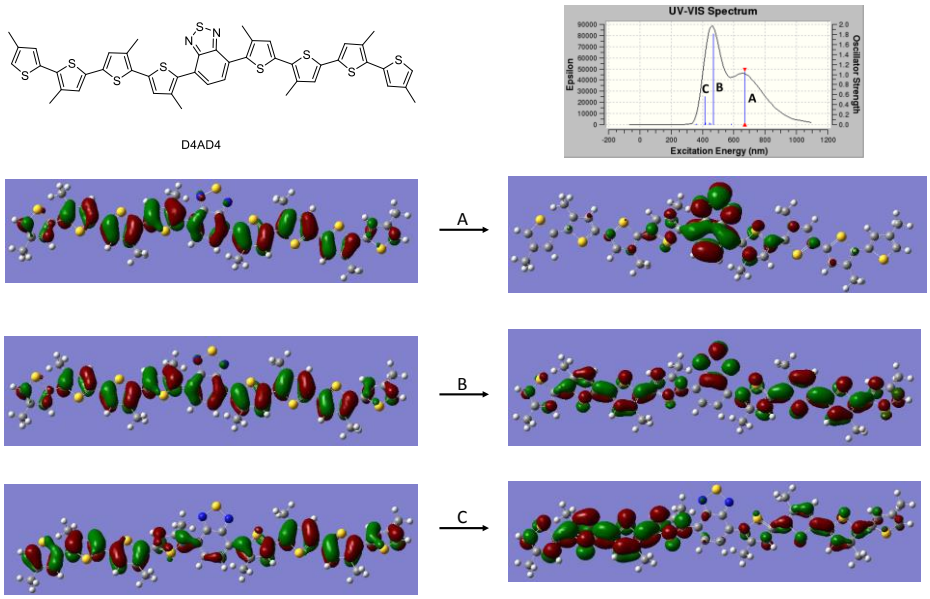

Figure S15. The simulated UV/vis spectra and Natural Transition Orbital analysis of D4AD4*. The first energy transition (A) is a donor-to-acceptor charge transfer transition. The second transition (B) is a mixture of donor-to-acceptor charge transfer transition and aromatic-to-quinoidal type transition. The third transition (C) is an aromatic-to-quinoidal type transition.

References

(1) Tanaka, S.; Tamba, S.; Tanaka, D.; Sugie, A.; Mori, A. *J. Am. Chem. Soc.* **2011**, *133* (42), 16734–16737.

(2) Tamba, S.; Tanaka, S.; Okubo, Y.; Meguro, H.; Okamoto, S.; Mori, A. *Chem. Lett.* **2011**, *40* (4), 398–399.

(3) Tkachov, R.; Senkovskyy, V.; Beryozkina, T.; Boyko, K.; Bakulev, V.; Lederer, A.; Sahre, K.; Voit, B.; Kiriy, A. *Angew. Chem. Int. Ed.* **2014**, *53* (9), 2402–2407.

(4) Lawrence, J.; Lee, S.-H.; Abdilla, A.; Nothling, M. D.; Ren, J. M.; Knight, A. S.; Fleischmann, C.; Li, Y.; Abrams, A. S.; Schmidt, B. V. K. J.; Hawker, M. C.; Connal, L. A.; McGrath, A. J.; Clark, P. G.; Gutekunst, W. R.; Hawker, C. J. *J. Am. Chem. Soc.* **2016**, *138* (19), 6306–6310.

(5) Zhang, Q.; Russell, T. P.; Emrick, T., *Chem. Mater.* **2007,** *19* (15), 3712–3716.

(6) Anant, P.; Lucas, N. T.; Jacob, J. *Org Lett* **2008**, *10*, 5533–5536.

(7) Zhang, L.; Colella, N. S.; Liu, F.; Trahan, S.; Baral, J. K.; Winter, H. H.; Mannsfeld, S. C. B.; Briseno, A. L. *J. Am. Chem. Soc.* **2013**, *135* (2), 844–854.